Illuminant color perception of spectrally filtered spotlights

Byung-Geun Khang

Helmholtz Institute, Utrecht University, Utrecht, The Netherlands

Qasim Zaidi

SUNY College of Optometry, New York, NY, USA

The color perceived to belong to the illumination of objects is often based on cues from the scene within which the objects are perceived, instead of being based on any view of the source itself. We present measurements of illuminant color estimation by human observers for moving, spectrally filtered spotlights. The results show that when only one illuminant is in the field of view, estimates of illuminant color are seriously biased by the chromaticities of the illuminated surfaces. When the surround of the spotlight is illuminated by a dimmer second light, spotlight matching moves toward veridical in most conditions. Simulations show that a gray-world model cannot be rejected as an adequate explanation for illuminant color estimation and provides as good a fit as a model that gives greater weights to the brightest surfaces. When the surrounding illuminant is brighter than the spotlight, the situation is similar to that of a moving filter. Spotlight matches are close to veridical, and the results can be fit by a model based on estimating both illuminants.

Keywords: illuminant color, color scission, color constancy, gray world, brightness weighting

Introduction

A color perception in the illumination mode always accompanies the perception of an object color, yet it is not referred to a definite volume in the illuminant mode, nor is it the perception of the volume color of the space in which the object color is perceived. It is a color perceived to belong to the illumination of the object based on clues from the scene within which the object is perceived instead of being based on any view of the source itself (Judd, 1961).

There are at least two reasons that illumination perception could be useful in everyday life. First, when coupled with memory, extracting the color of the illuminant may itself be functional (e.g., in estimating weather or time of day) (Zaidi, 1998). Second, several authors have conjectured that an estimate of the illuminant may be necessary to see surfaces as having constant colors (e.g., Helmholz, 1962; Kardos, 1929; Katz, 1935; Koffka, 1935; Woodworth, 1938) and constant three-dimensional (3D) shapes (Adelson & Pentland, 1991).

Many models have been proposed for illuminant color estimation or classification: gray world models (Buchsbaum, 1980; Land, 1986), specular highlights (Lee, 1986; D'Zmura & Lennie, 1986; Lehmann & Palm, 2001), low-dimensional linear basis spectra (Maloney & Wandell, 1986; Tominaga & Wandell, 1989; Brainard & Wandell, 1991; D'Zmura & Iverson, 1993, 1994; Brainard & Freeman, 1997), sensor gamut matching (Forsyth, 1990; Finlayson, Hubel, & Hordley, 1997; Tominaga, Ebisui, & Wandell, 2001), heuristics-based color transformations (Zaidi, 1998, 2001), and luminance-chromaticity correlations (MacLeod & Golz, 2003; Golz & MacLeod, 2002). Other than Linnell and Foster (2002), Yang and Maloney (2001), and this study, experimental studies on illuminant perception have been restricted to achromatic worlds (Kardos, 1929; Beck, 1959; Gilchrist & Jacobsen, 1984; Rutherford & Brainard, 2002).

In this study, we have examined how observers extract the colors of spectrally filtered spotlights that are cast on backgrounds formed from different variegated sets of materials. In an asymmetric spotlight matching technique, observers were asked to match the color of a Standard spotlight moving on spectrally selective materials by adjusting the color of a Match spotlight moving over materials with uniform reflectance spectra (Figure 1). Because the illuminated materials are different under the two spotlights, this match cannot be accomplished by point-by-point color matching, but instead requires matching the extracted colors of the illuminants. Three separate experiments were examined in this work. In the first, the spotlight was the only illuminant in the field of view (Figure 1, top) (i.e., the only objects visible were those that fell under the spotlight). In the second and third experiments, the objects not illuminated by the spotlight were visible under a dim (Figure 1, middle) and a bright (Figure 1, bottom) equal-energy illuminant, respectively. The same materials were used in all three experiments, and were simulated as matte flat surfaces. The first experiment was used to examine estimation strategies for illuminant color when only one illuminant was in the field of view, in the absence of cues provided by highlights, shading, and shadows. The results show that illuminant color estimates are systematically biased by the spectral reflectances of the illuminated surfaces. The second experiment examined how cues from a second illuminant

doi:10.1167/4.9.2 Received February 5, 2004; published August 24, 2004 ISSN 1534-7362

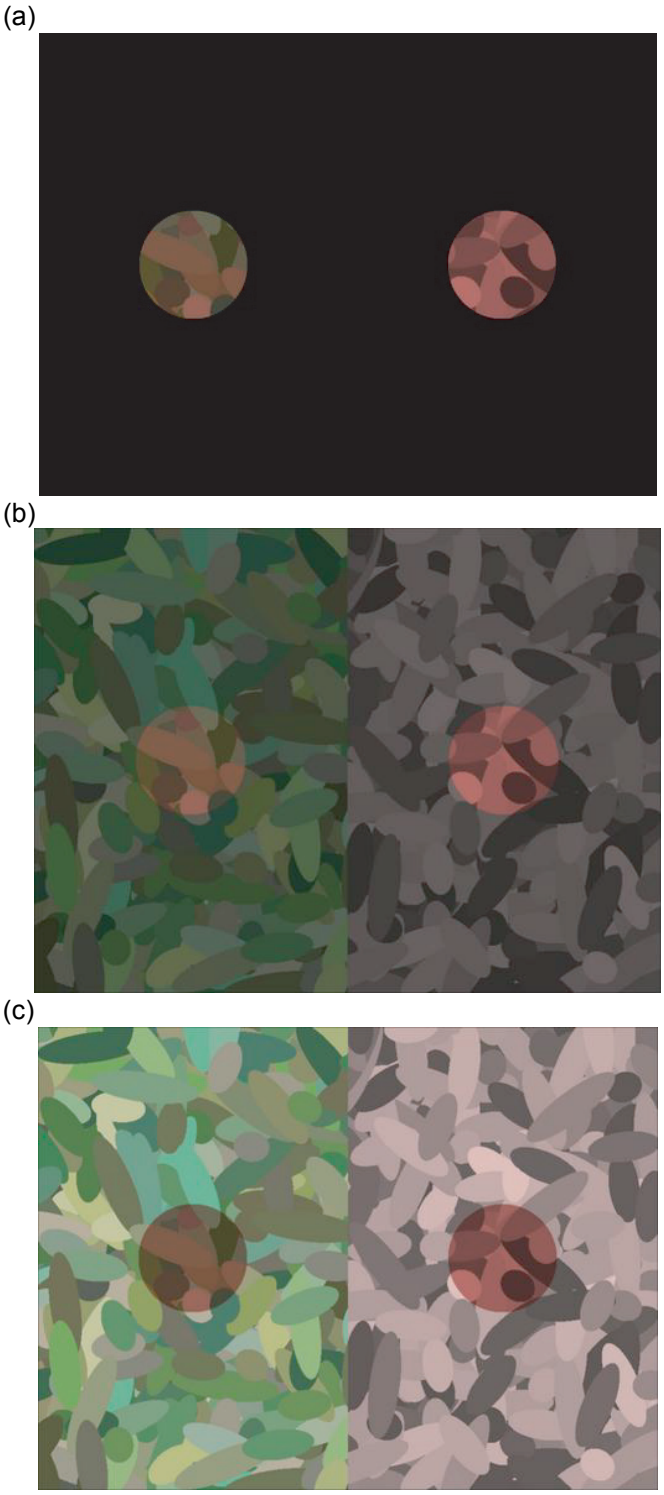

Figure 1. (a). Experiment 1: Red spotlight cast on green-yellow materials (left) and the same red spotlight on gray materials (right). Observers were asked to estimate the color of the spotlight on chromatic materials and to match it by adjusting the spectrum of the spotlight on gray materials. (b). Experiment 2: The same red spotlights on the same materials in the presence of dim illumination on the surround. (c). Experiment 3: The same red spotlights on the same materials in the presence of brighter illumination on the surround. To see the spotlights moving, click on each photo.

in the field of view are used to improve illuminant color estimates. The third experiment (Khang & Zaidi, 2002) examined the condition where the surrounding illuminant is brighter than the spotlight. Under this condition, which is akin to filter matching, illuminant color estimates are near veridical in most conditions.

Methods

Surfaces

The Standard spotlight moved over one of four sets of 40 materials from single quadrants of MacLeod-Boynton (1979) color space, or a fifth set equally balanced across quadrants, chosen from 4,824 reflectance functions of flowers, leaves, fruits (Chittka, Shmida, Troje, & Menzel, 1994), natural and man-made objects (Vrhel, Gershon, & Iwan, 1994), Munsell color chips (Lenz, Osterberg, Hiltunen, Jaaskelainen, & Parkkinen, 1996), and animal skins (Marshall, 2000). Match spotlights moved over a sixth set of 40 materials with uniform reflectance spectra whose magnitudes of reflectance were set to match the mean reflectance of each of the 40 materials of the balanced chromatic set. Figure 2 shows MacLeod-Boynton chromaticities of the six sets of materials under Equal Energy light. The reflectance spectra of the six sets of materials are shown in Khang and Zaidi (2002). Materials were simulated as randomly sized, oriented, and overlapping ellipses (Figure 1). The length of

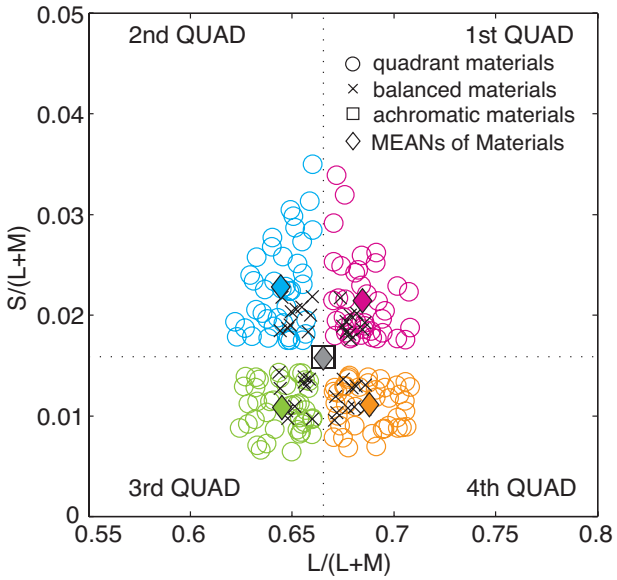

Figure 2. MacLeod-Boynton chromaticities (under equal energy light) of the 240 materials used, which consisted of 6 sets of 40 materials, 4 sets of chromatic materials from each quadrant, 1 set of balanced chromatic materials, and 1 set of achromatic materials. Colored diamonds indicate mean of each quadrant's materials, while the square and the gray diamond at the intersection of the horizontal and vertical dotted lines (Equal Energy light) represent both the achromatic materials and the mean of the balanced chromatic materials.

the major axis was set between 2.20° to 6.59° and the length of the minor axis was set at 1.83°. Seven different spatial layouts were drawn in image memory, and a different layout was randomly chosen as the background on each trial. There were 576 ellipses per layout; some ellipses were partially or completely occluded by others. Materials were randomly assigned to ellipses on each trial.

Spotlights

Each spotlight was simulated as overlaying a circular region with a diameter of 6.6° and moving along a circular trajectory with a diameter of 6.6°. Figure 3 shows the spectral radiance functions of the seven spotlights. These functions were obtained by double-passing equal energy light through one of six Kodak CC30 (Eastman Kodak, Rochester, NY) color filters (Red, Green, Blue, Yellow, Magenta, and Cyan) (KodakCC30, 1962) or through a Neutral density filter with 70% transmittance.

Equipment

All stimulus presentations and data collection were computer controlled. Stimuli were displayed on the 36° x 27° screen (1024 x 768 pixels) of a Nokia Multigraph 445Xpro color monitor with refresh rate of 70 frames/s at a viewing distance of 60 cm. Images were generated by a Cambridge Research Systems Visual Stimulus Generator (CRS VSG2/3), running in a 400-MHz Pentium II-based system. Through the use of 12-bit digital-analog converters, after gamma correction, the VSG2/3 was able to generate 2861 linear levels for each gun. Any 256 combinations of the three guns could be displayed during a single frame. By cycling through precomputed lookup tables, we were able to update the entire display each frame. A Spectra-Scan PR-704 photospectroradiometer was used to measure complete spectra for the three phosphors. Phosphor chromaticities CIE (x, y) and luminances measured at the maximum luminance were (0.60, 0.34) and 11.6 cd/m^2 for the R-gun, (0.28, 0.60), 34.2 cd/m^2 for the G-gun, and (0.15, 0.07) and 4.8 cd/m^2 for the B-gun.

Rendering

A material with reflectance $\theta_i(\lambda)$ seen under an illuminant with spectrum $P_j(\lambda)$ was rendered by first calculating cone absorptions L_{ij}, M_{ij}, and S_{ij}, for the Long-, Middle-, and Short-wavelength sensitive cones (Smith & Pokorny, 1975):

$$L_{ij} = \int P_j(\lambda)\cdot\theta_i(\lambda)\cdot L(\lambda)d\lambda \quad (1)$$

$$M_{ij} = \int P_j(\lambda)\cdot\theta_i(\lambda)\cdot M(\lambda)d\lambda \quad (2)$$

$$S_{ij} = \int P_j(\lambda)\cdot\theta_i(\lambda)\cdot S(\lambda)d\lambda \quad (3)$$

Cone absorptions for materials lit by the spectral spotlights (Experiments 1, 2, and 3), and surrounding materials exposed under equal-energy light (Experiments 2 and 3) were transformed to gun values and displayed on the screen.

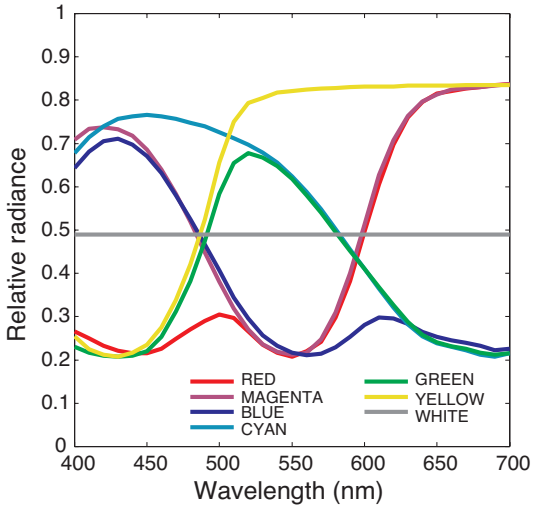

Figure 3. Spectra of seven spotlights simulated in the three experiments.

Procedure

On each trial, one of the five sets of simulated chromatic materials was used as the background on the left half of the screen, and the achromatic set was used as the background on the right half. The Standard and Match spotlights were simulated as illuminating the chromatic and achromatic materials, respectively. The Standard spotlight simulated one of the seven spectra in Figure 3. Observers were asked to imagine how the Standard spotlight on the chromatic materials would look if it were presented on the achromatic materials and to match the two spotlights by adjusting the color of the Match spotlight. Two toggle switches varied the spectrum of the Match spotlight $P_m(\lambda)$ inside the convex hull formed by the linear combination of the Standard spotlight $P_t(\lambda)$, the Equal Energy spotlight $P_n(\lambda)$, and the two spotlights $P_{t-1}(\lambda)$ and $P_{t+1}(\lambda)$ with spectra closest to the Standard spotlight (e.g., Magenta and Yellow for the Red Standard spotlight):

$$P_m(\lambda) = \{P_t(\lambda)[1-\Delta_c] + \Delta_c P_{t-1}(\lambda)\}[1-\Delta_n] + \Delta_n P_n(\lambda) \quad \text{for } 0 \le \Delta_c \le 1 \quad (4)$$

$$P_m(\lambda) = \{P_t(\lambda)[1+\Delta_c] - \Delta_c P_{t+1}(\lambda)\}[1-\Delta_n] + \Delta_n P_n(\lambda) \quad \text{for } -1 \le \Delta_c \le 0 \quad (5)$$

The first switch varied Δ_c between –1 and +1, adjusting the hue of the Match spotlight. The second switch adjusted Δ_n from 0 up to the positive value greater than 1 where all of the overlaid achromatic materials remained displayable, adjusting the saturation of the Match spotlight. Δ_c and Δ_n were initially assigned random values on each trial. Stimuli on each trial were presented until the observer had finished the adjustment of the Match spotlight.

There were 35 material and Standard spotlight combinations (five sets of background materials and seven Standard spotlights) presented in random order. For each condition, 5 observations were made per observer in Experiment 1, 8 in Experiment 2, and 15 in Experiment 3.

Observers

All observers had normal or corrected-to-normal visual acuity and normal color vision. Experiments 1, 2, and 3 were run in reverse chronological order. Four observers participated in Experiments 2 and 3; only three of these observers were able to participate in Experiment 1. In both experiments, observer BK was the first author. The other observers were not informed about the purposes of the experiment until after completion of all measurements.

Experiment 1: Spotlight matching with dark surrounds

The simulation (Figure 1, top) gave a vivid impression of a spotlight moving over colored materials in a dark scene, and as different objects were successively illuminated, the display provided rich information about the color of the spotlight.

Using Equations 4 and 5 and the values of Δ_c and Δ_n set by the observer, each match can be converted into an illuminant spectrum, and compared with the illuminant spectrum of the Standard spotlight. Because the Match spotlight overlays achromatic surfaces, any spotlight that is metameric with it will also provide a good match to the Standard spotlight. This statement reflects the fact that observers do not have access to spectra but to functions of cone-absorptions that lead to perceived colors, and that all metameric lights will appear chromatically identical on the same achromatic surfaces. In addition, radiance versus wavelength does not provide a perceptually relevant metric to compare deviations from veridicality. We have, therefore, used chromaticities to compare Match spotlights to Standard and predicted spotlights.

There is no diagram that accurately represents color appearance, so to provide concise and physiologically tractable descriptions of the patterns of results, we have used MacLeod-Boynton chromaticity coordinates (L/(L+M), S(L+M)). In Figure 4, each X represents the chromaticity of the Standard spotlight. Each X thus represents veridical illuminant color estimation (i.e., data points will overlap the X when the Match spotlight spectrum is isomeric or metameric to the Standard spotlight spectrum). Clustered near each X are filled circles and diamonds representing the mean chromaticities of the Match spotlights. The circles and diamonds are color-coded similar to Figure 2 to represent the chromatic backgrounds. The results are systematic and similar for the three observers. On balance, the gray disks appear closest to the Xs, indicating that matches were most accurate to Standard spotlights on Balanced materials (i.e., when the two sets of background surfaces had the same mean chromaticity despite vastly different chromatic variances). The points for the biased backgrounds show substantial deviations from veridical.

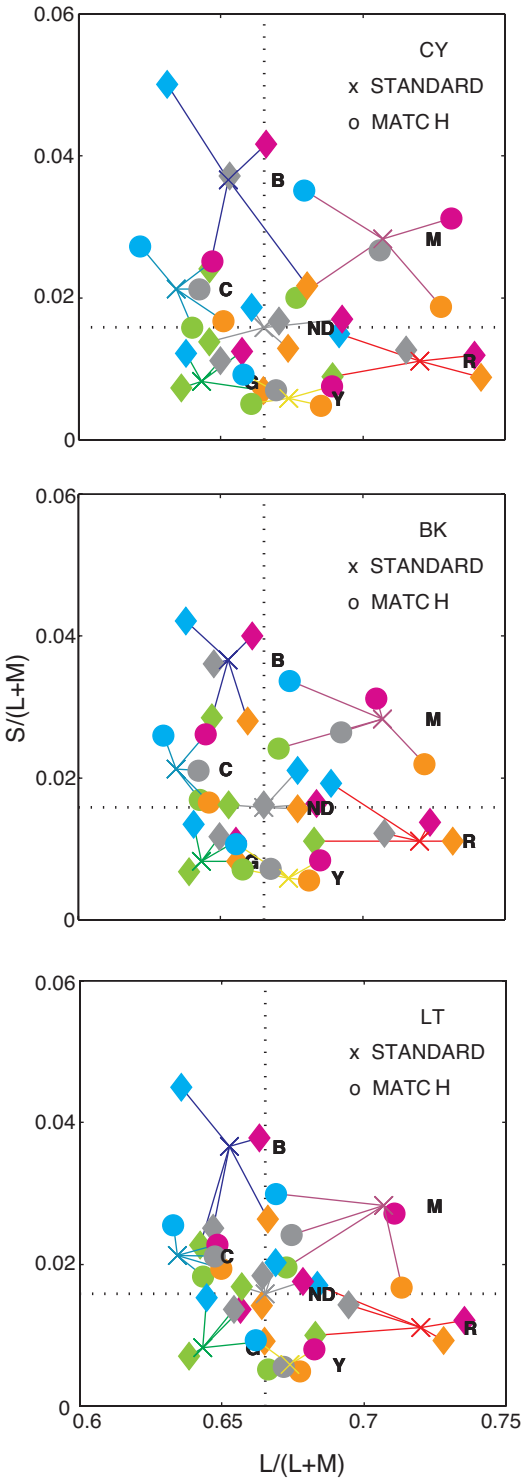

Figure 4. Chromaticities of the Standard (x) (R,M,B,C,G,Y,ND) and mean Match spotlights (o) for each of three observers. Colors of the circles indicate chromatic background conditions: gray = balanced, purple = 1st quadrant, cyan = 2nd quadrant, green = 3rd quadrant, and orange = 4th quadrant.

Because the patterns formed by the colored disks in Figure 4 are similar for all three observers, we combined the results and calculated means over all observers. In Figure 5, each of the five panels represent matches for all seven Standard spotlights on one of the five chromatic backgrounds, indicated as BALANCED or QUAD #. Average chromaticities of the mean Match spotlights (empirical matches) are shown as plusses (+), and enclosed by ellipses that indicate ±1 *SD* along two axes: the axis of chromaticity variation due to Δ_n and the chromatic axis orthogonal to this variation (scatter plots of all matches supported these axes as representative of the variance in the matches). Xs represent the chromaticity of the Standard spotlight (veridical matches). Symbols are coded according to the color of the Standard spotlight. The diamonds in each panel represent the mean chromaticity of the background surfaces. In the panel for the chromatically balanced background, the Xs fall on or inside the ±1 *SD* ellipses, and the mean matches deviate from veridical toward the achromatic point (intersection of dashed horizontal and vertical lines). For the biased backgrounds, very few of the ellipses for the empirical matches contain the corresponding Xs. The mean empirical matches deviate from the veridical predominantly in the same direction as the mean background chromaticity deviates from the achromatic point, suggesting a systematic biasing effect of background chromaticities on illuminant estimation. This bias is the motivation for the models presented in the next section.

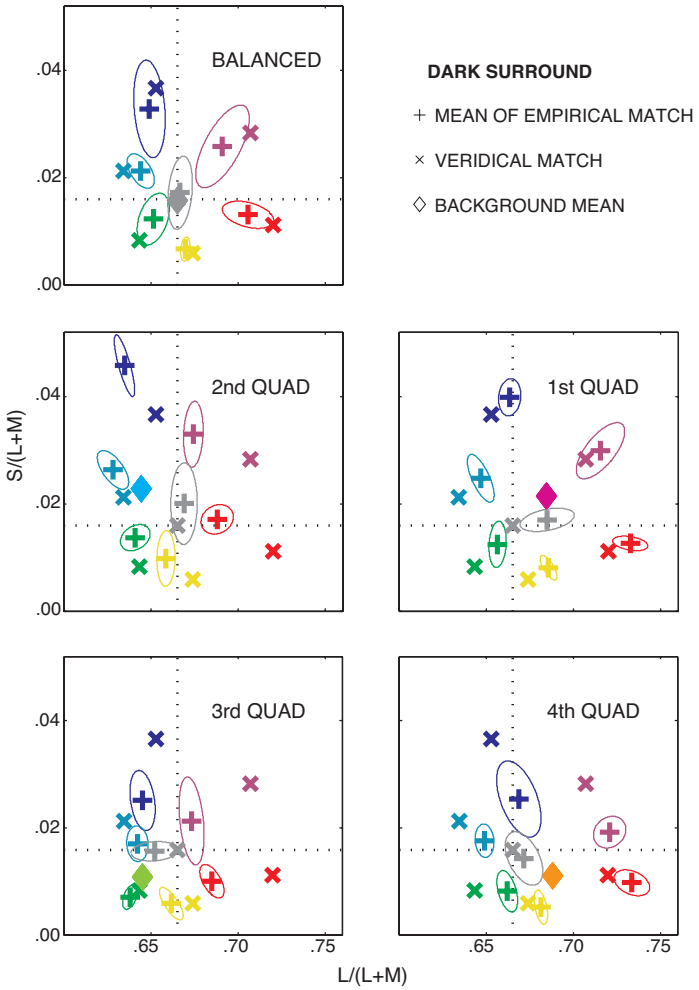

Figure 5. Chromaticities of the Standard spotlights (x) and mean Match spotlights (+) averaged over observers enclosed by ellipses showing 1 *SD*. Xs indicate veridical matches.

Model 1: Color estimation for single illuminants

The models for illuminant color estimation that are listed in the "Introduction" could be implemented as neural or cognitive strategies, based on the information available from the displays. In the simulation of flat matte surfaces under a single spatially uniform illuminant, the color information available from each material is the triple of cone-absorptions given by Equations 1-3, and retinal and later neural transformations of these inputs. If illuminant estimation requires statistics to be pooled over an extended region, then it is likely to involve cortical processes that use transformed values of cone-absorptions (Lennie, Krauskopf, & Sclar, 1990; Kiper, Fenstemaker, & Gegenfurtner, 1997; Gegenfurtner, Kiper, & Levitt, 1997). The models proposed in this work are essentially weighted linear combinations of cone absorptions, but these could easily be transformed to higher level models. The simplest model is the gray-world model, according to which estimates of cone-absorptions corresponding to the illuminant spectrum on the chromatic-background side, $\left[L_c(\hat{P}_j)\, M_c(\hat{P}_j)\, S_c(\hat{P}_j)\right]$, are obtained by taking the means of all the cone-absorptions:

$$L_c(\hat{P}_j) = \sum_i \int P_j(\lambda)\cdot\theta_i(\lambda)\cdot L(\lambda)\,d\lambda \qquad (6)$$

$$M_c(\hat{P}_j) = \sum_i \int P_j(\lambda)\cdot\theta_i(\lambda)\cdot M(\lambda)\,d\lambda \qquad (7)$$

$$S_c(\hat{P}_j) = \sum_i \int P_j(\lambda)\cdot\theta_i(\lambda)\cdot S(\lambda)\,d\lambda \qquad (8)$$

The subscripts *c* and *a* will be used to denote the chromatic and achromatic sides, respectively, and caps will denote estimated quantities. It is apparent from these equations that if $\sum_i \theta_i(\lambda)$ is a uniform spectrum, then $Lc(\hat{P}_j) = L(P_j)$, $Mc(\hat{P}_j) = M(P_j)$, $Sc(\hat{P}_j) = S(P_j)$. In other words, the estimate will be veridical when the background is balanced, but not when it is biased.

Models for illuminant estimation, however, should incorporate the fact that high-intensity regions of scenes potentially contain more illuminant color information than

do low-intensity regions. Tominaga et al. (2001) present the following thought experiment: The image of a black surface will have close to zero sensor responses under any illuminant, and its chromaticity will be a function of random noise; whereas, a white surface will map reliably to the chromaticity corresponding to the illuminant spectrum. Hence, combining the two measurements will produce a worse estimate of the illuminant than using the bright region alone. In a simulation study of black-body illuminants, Tominaga et al. (2001) demonstrated that sensor responses from the brightest intensity regions were most diagnostic in classifying illuminants of different color temperature. Golz and MacLeod (2002) have suggested that correlation between chromaticity components of scene objects (e.g., luminance versus redness) could provide a clue for extracting illuminant color. Tominaga et al. (2001) simulation results would argue that due to random noise for the darker surfaces, statistics based on the brightest regions would provide a better estimate than the correlation. In devising the model presented below, we have used this justification, plus the consideration that taking a spatial sum is a simpler neural process than extracting a correlation.

We have implemented these ideas by generalizing the gray-world model to incorporate weighting by the luminance of each spotlighted material with the luminance raised to a positive power:

$$L_c\left(\hat{P}_j\right) = \sum_i V_{ij}^{\,n} \int \theta_i(\lambda)\cdot P_j(\lambda)\cdot L(\lambda)\,d\lambda \qquad (9)$$

$$M_c\left(\hat{P}_j\right) = \sum_i V_{ij}^{\,n} \int \theta_i(\lambda)\cdot P_j(\lambda)\cdot M(\lambda)\,d\lambda \qquad (10)$$

$$S_c\left(\hat{P}_j\right) = \sum_i V_{ij}^{\,n} \int \theta_i(\lambda)\cdot P_j(\lambda)\cdot S(\lambda)\,d\lambda \qquad (11)$$

where for the CIE $V(\lambda)$ function

$$V_{ij} = \int P_j(\lambda)\cdot\theta_i(\lambda)\cdot V(\lambda)\,d\lambda \qquad (12)$$

If $n = 0$, the weighted model is identical to the gray-world model. As n increases, the brighter materials are weighted more, and at $n=\infty$, only cone catches from the brightest material are effective in the model.

The linking hypothesis for the spotlight matches is that the observer first extracts $\left[L_c\left(\hat{P}_j\right) M_c\left(\hat{P}_j\right) S_c\left(\hat{P}_j\right)\right]$ from the chromatic-background side using the calculations in Equations 9-11, then sets Δ_c and Δ_n to achieve a spectrum $P_m(\lambda)$ on the achromatic side, so that

$$L_a\left(P_m\right) = L_c\left(\hat{P}_j\right) \qquad (13)$$

$$M_a\left(P_m\right) = M_c\left(\hat{P}_j\right) \qquad (14)$$

$$S_a\left(P_m\right) = S_c\left(\hat{P}_j\right). \qquad (15)$$

The predicted values of $\left[L_a\left(P_m\right), M_a\left(P_m\right), S_a\left(P_m\right)\right]$ were converted to MacLeod-Boynton coordinates and tested against the empirical matches. In Figure 6 the empirical means (pluses) and the ±1 *SD* ellipses are replotted on the same axes as Figure 5. The other symbols near the plusses show the model predictions for $n = 0$ (inverted triangles representing the gray world model) and $n = 10$ (upright triangle representing the brightness weighting model). Note that there are no free parameters in either model. The value of n that determines the selectivity of brightness weighting is fixed for each model. Two considerations apply in testing the models. First, any prediction that is more than 2 *SD* from the mean can be rejected as a good fit. By this criterion, hardly any of the predictions from either model are rejected. However, given the large sizes of the ellipses for this data set, this test is not very selective. The second consideration is that the pattern of predictions from a model should be close to the pattern of the empirical means. Both models do fairly well in this regard, and the brightness-weighted model ($n = 10$) does not provide a sig-

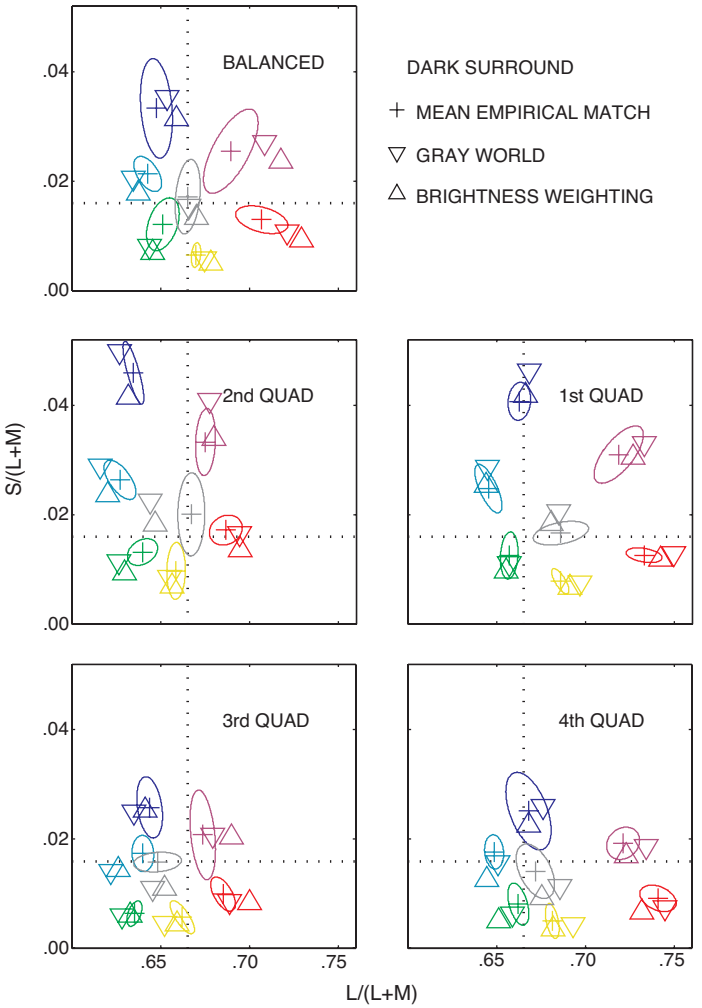

Figure 6. Mean chromaticities of the Match spotlights (+), and predictions from a gray-world model (▽), and a model that gives great weight to the brightest materials (△).

nificantly better explanation for illuminant color estimation. The predictions for $n = 1$ were very similar to those for $n = 0$, and the predictions for $n = 100$ were very similar to those for $n = 10$. The predominant discrepancy seems to be that the matched chromaticity is less saturated than the predicted chromaticity. This may be due to the desaturating effects of adaptation to chromatic variations, which, in this study, are present only on the side with the Standard filter (Krauskopf , Williams, & Heeley, 1982; Webster & Mollon, 1997; Zaidi, Spehar, & DeBonet, 1997, 1998). This possibility points out that a proper brightness-weighting model should incorporate better estimates of the brightness and color appearance of different surfaces, and both estimates are likely to be nonlinear functions of cone-absorptions. Equations 9-11 are just an approximation to this class of models. Note that, for the biased backgrounds, the model predictions are not good estimates of the veridical matches shown in Figure 5. It is worth pointing out that for $n = \infty$, we are explicitly not claiming that the brightest surface appears as the illumination source. Identification of the illumination source depends on geometric factors like fuzzy borders (Zavagno, 1999), which are not present in our displays. In their gamut matching simulations, Tominaga et al. (2001) found it useful to scale the intensity of all images to keep them within similar ranges; in the human visual system, retinal processes like photoreceptor adaptation and center surround receptive fields provide automatic intensity scaling for later visual processing.

Experiment 2: Spotlight matching in the presence of a dimmer second illuminant

It should not be surprising that observers were not able to make veridical matches in most of the conditions of Experiment 1. The only information present in the stimuli is the set of cone absorptions from materials illuminated by the spotlight, and statistics derived from these cone absorptions cannot separate illuminant from material properties without ancillary assumptions. Therefore, these statistics will only lead to veridical illuminant estimates for the very few sets of material reflectances that satisfy these assumptions. In many natural conditions, however, more than one illuminant is present on a scene, and if the two illuminants fall on similar sets of materials, this provides additional information about the relative spectra of the two illuminants (Zaidi, 1998, 2001). There are a variety of such situations, one of which is illustrated in Figure 1 (middle), and consists of a circumscribed, bright spotlight falling on a scene lit by a distinct dimmer background illuminant. When the spotlight was moved around, there was a distinct scission between the moving colored spotlight and the stationary dimly illuminated background. To provide a comparison with the results of Experiment 1, the spotlight regions were identical to the overlaid regions in Experiment 1; in fact, all aspects of Experiment 2 were identical to those of Experiment 1 except that the regions surrounding the moving spotlight were illuminated by an equal energy light of intensity equal to 20 % of that passing through the spotlight filter.

The mean empirical matches of spotlights are plotted on the MacLeod-Boynton diagram (Figure 7) along with the veridical matches, in the same manner as Figure 5. The corresponding results from Experiment 1 are included for comparison. It is clear that the presence of the second illuminant affects spotlight matches that are now closer to veridical in the majority of instances. The cues from the second illuminant in the field of view, that are used to improve illuminant color estimates, are the motivation for the models presented in the next section.

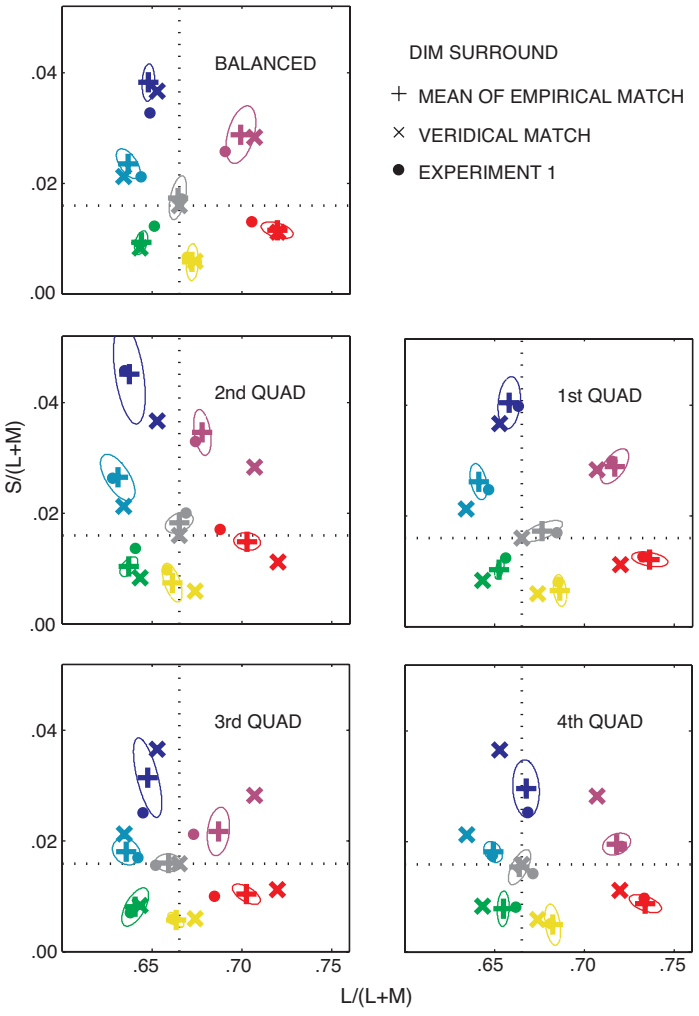

Figure 7. Chromaticities of the Standard spotlights (x) and the mean Match spotlights (+). Xs indicate veridical matches. Results of Experiment 1 are repeated for comparison as filled dots.

Model 2: Color estimation for spotlights added to a more extensive second illuminant

The increased accuracy of spotlight matches in Experiment 2 compared to Experiment 1 demonstrates that observers are utilizing the extra information available from the exposed regions. It is clear that the simple illuminant estimation models described earlier will not provide good fits to the data from Experiment 2. We conjecture that observers first estimate the illuminant $E_c(\lambda)$ on the exposed region of the chromatic background, and then assume that the spotlight is added on to the dim light, so that $P_j(\lambda)$ is equal to $F_j(\lambda)+E_c(\lambda)$, where $F_j(\lambda)$ is the added spectrum. The observer can thus estimate $\left[L_c(\hat{F}_j),\ M_c(\hat{F}_j),\ S_c(\hat{F}_j)\right]$ from $\left[L_c(\hat{P}_j)-L_c(\hat{E}_c),\ M_c(\hat{P}_j)-M_c(\hat{E}_c),\ S_c(\hat{P}_j)-S_c(\hat{E}_c)\right]$. $\left[L_c(\hat{P}_j),\ M_c(\hat{P}_j),\ S_c(\hat{P}_j)\right]$ are estimated from Equations 9-11, and for E, a uniform spectrum:

$$L_c(\hat{E}_c)=\sum_i {V_{iE}}^n \int \theta_i(\lambda)\cdot E(\lambda)\cdot L(\lambda)d\lambda \quad (16)$$

$$M_c(\hat{E}_c)=\sum_i {V_{iE}}^n \int \theta_i(\lambda)\cdot E(\lambda)\cdot M(\lambda)d\lambda \quad (17)$$

$$S_c(\hat{E}_c)=\sum_i {V_{iE}}^n \int \theta_i(\lambda)\cdot E(\lambda)\cdot S(\lambda)d\lambda \quad (18)$$

where

$$V_{iE}=\int \theta_i(\lambda)\cdot E(\lambda)\cdot V(\lambda)d\lambda\,. \quad (19)$$

The linking hypothesis for the spotlight matches is that the observer sets $P_m(\lambda)$ on the achromatic side, so that

$$L_a(F_m)=L_c(\hat{F}_j) \quad (20)$$

$$M_a(F_m)=M_c(\hat{F}_j) \quad (21)$$

$$S_a(F_m)=S_c(\hat{F}_j) \quad (22)$$

where

$$L_a(F_m)=L_a(P_m)-L_a(E_a) \quad (23)$$

$$M_a(F_m)=M_a(P_m)-M_a(E_a) \quad (24)$$

$$S_a(F_m)=S_a(P_m)-S_a(E_a). \quad (25)$$

This implies that cone-absorptions for P_m can be obtained by

$$L_a(P_m)=L_c(\hat{P}_j)-L_c(\hat{E}_c)+L_a(\hat{E}_a) \quad (26)$$

$$M_a(P_m)=M_c(\hat{P}_j)-M_c(\hat{E}_c)+M_a(\hat{E}_a) \quad (27)$$

$$S_a(P_m)=S_c(\hat{P}_j)-S_c(\hat{E}_c)+S_a(\hat{E}_a) \quad (28)$$

where the cone estimates for E_a the illuminant on the achromatic side are

$$L_a(\hat{E}_a)=\sum_i {V_{iaE}}^n \cdot \int r\cdot E(\lambda)_i \cdot L(\lambda)d\lambda \quad (29)$$

$$M_a(\hat{E}_a)=\sum_i {V_{iaE}}^n \cdot \int r_i\cdot E(\lambda)\cdot M(\lambda)d\lambda \quad (30)$$

$$S_a(\hat{E}_a)=\sum_i {V_{iaE}}^n \cdot \int r_i\cdot E(\lambda)\cdot S(\lambda)d\lambda \quad (31)$$

where

$$V_{iaE}=\int r_i\cdot E(\lambda)\cdot V(\lambda)d\lambda \quad (32)$$

and r_i are the reflectances of the achromatic materials.

The predicted values of $\left[L_a(P_m),\ M_a(P_m),\ S_a(P_m)\right]$ were converted to MacLeod-Boynton chromaticities and compared to the empirical matches from Figure 7, which are replotted as plusses on the same axes in Figure 8. The other symbols near the plusses show the model predictions for $n = 0$ and 10 (downward and upward pointing triangles, respectively). Note that there are no free parameters in this model. The value of n, which determines the selectivity of brightness weighting, is fixed for each model. Many of the points from the gray-world ($n = 0$) hypothesis come close to the data points. The predictions for $n = 1$ were very similar to those for $n = 0$. The predictions of the brightness-weighted model ($n = 10$) do not differ greatly from the gray-world model. The predictions for $n = 100$ were very similar to that for $n = 10$. The 1 *SD* ellipses are smaller for Experiment 2 than for Experiment 1 (possibly due to a larger number of repetitions per condition), and in almost all of the cases, neither of the two models can be rejected. It is worth pointing out that Model 2 reduces to Model 1 when the surround illuminant $E(\lambda)$ is equal to zero.

Experiment 3: Spotlight matching in the presence of a brighter background

The simulations in the first two experiments evoked percepts of spotlights moving over fixed backgrounds. The presence of a background illuminant moved spotlight matches toward veridical, but the shift was small in many cases. We were interested in the effects of a brightly lit surround on spotlight estimation. As a third condition, we simulated circumscribed, bright spotlights falling on scenes

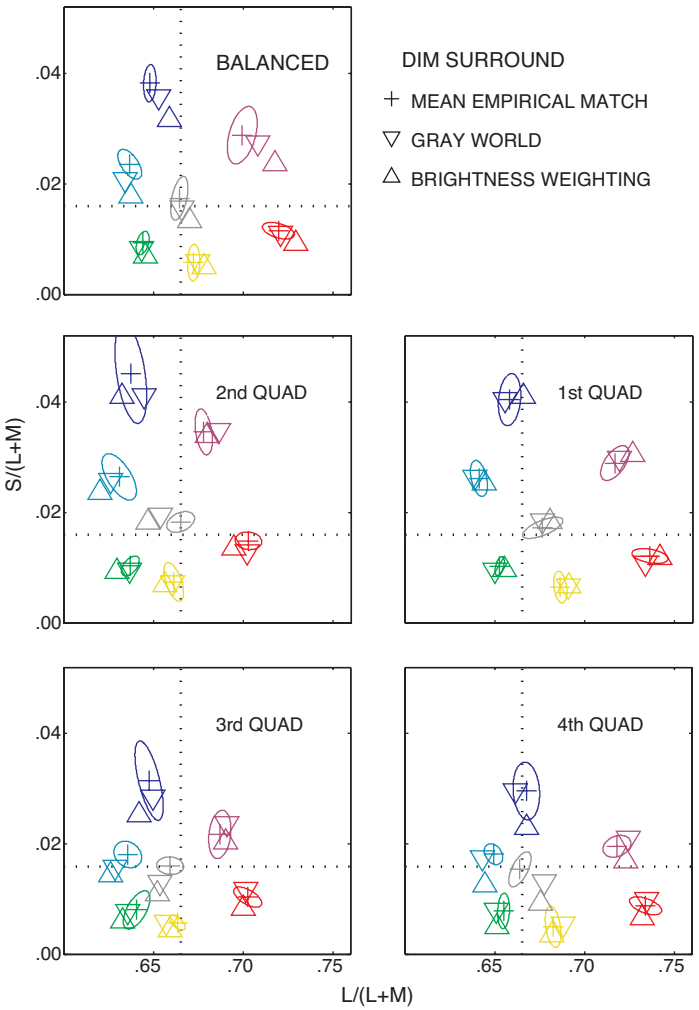

Figure 8. Mean chromaticities of the Match spotlights (+), and predictions from a gray-world model (▽), and a model that gives greater weight to the brightest materials (△). Note that these models are generalizations of the ones in Figure 6.

lit by a bright background illuminant (Figure 1, bottom). To provide a comparison with the results of Experiment 1, the spotlight regions were identical to the overlaid regions in Experiment 1, and the exposed regions were illuminated by an equal energy light of intensity equal to that passing through the spotlight filter.

This experiment was run by Khang and Zaidi (2002) to measure matching accuracy for filters. Because all aspects of the filter matching experiment except the presence of illumination in the surround regions were identical to those of the spotlight matching experiment, the filter-matching experiment can also be conceived of as spotlight matching in the presence of a second illuminant. We replot the data here (Figures 9 and 10) in the same manner as for the spotlight experiments, and use them to test a model based on estimating illuminant colors.

The mean empirical matches of spotlights are plotted on the MacLeod-Boynton diagram (Figure 9) along with the veridical matches, in the same manner as Figure 5. The corresponding results from Experiment 1 are included for comparison. It is clear that the presence of the bright, second illuminant has enabled observers to make matches that are close to veridical in the majority of instances. For the biased backgrounds, deviations of the Match spotlight from the Standard tended to occur along the line connecting the Xs for the Standard and the achromatic point, indicated by the intersection of the horizontal and vertical dashed lines (i.e., discrepancies in spotlight matching occurred in saturation rather than hue). The largest departures from accurate estimation occur when the Standard spotlight overlays a set of chromatic materials whose reflectance spectra are most dissimilar in shape to the spectrum of the Standard spotlight (e.g., Green spotlight on the 1st quadrant [red-blue] materials, Red on the 2nd quadrant [green-blue], Magenta on the 3rd quadrant [green-yellow] materials, and Cyan on the 4th Quadrant [red-yellow]). The results of this experiment show that the cues from the second illuminant in the field of view are used to improve illuminant color estimates to near veridical. These cues are the motivation for the models presented in the next section.

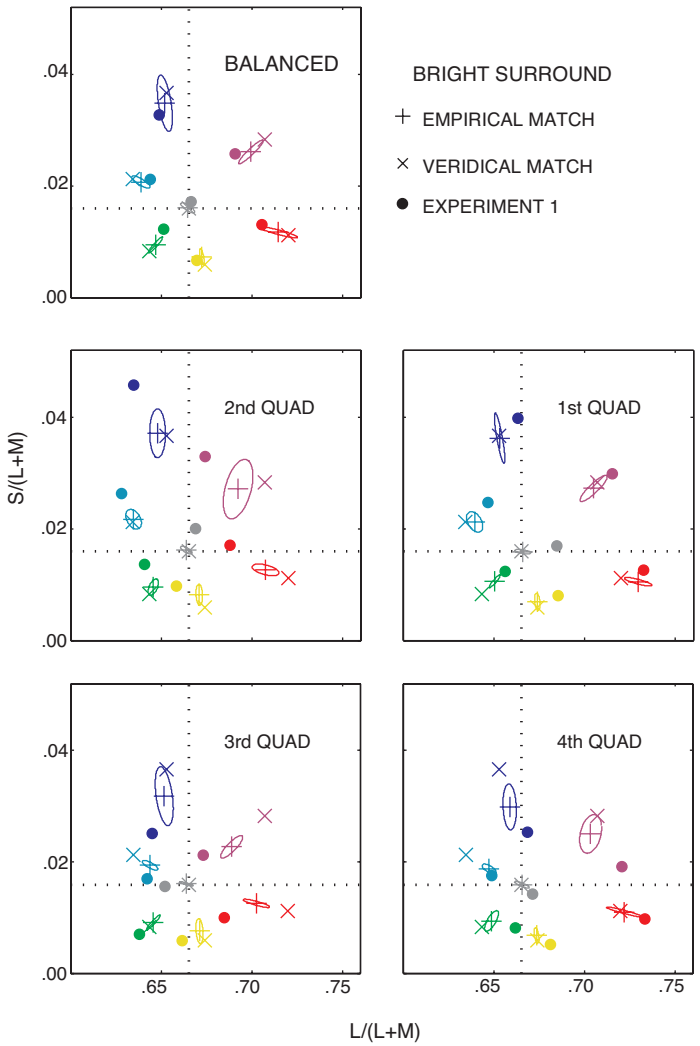

Figure 9. Chromaticities of the Standard spotlights (x) and the mean Match spotlights (+). Xs indicate veridical matches. Results of Experiment 1 are repeated for comparison as filled dots.

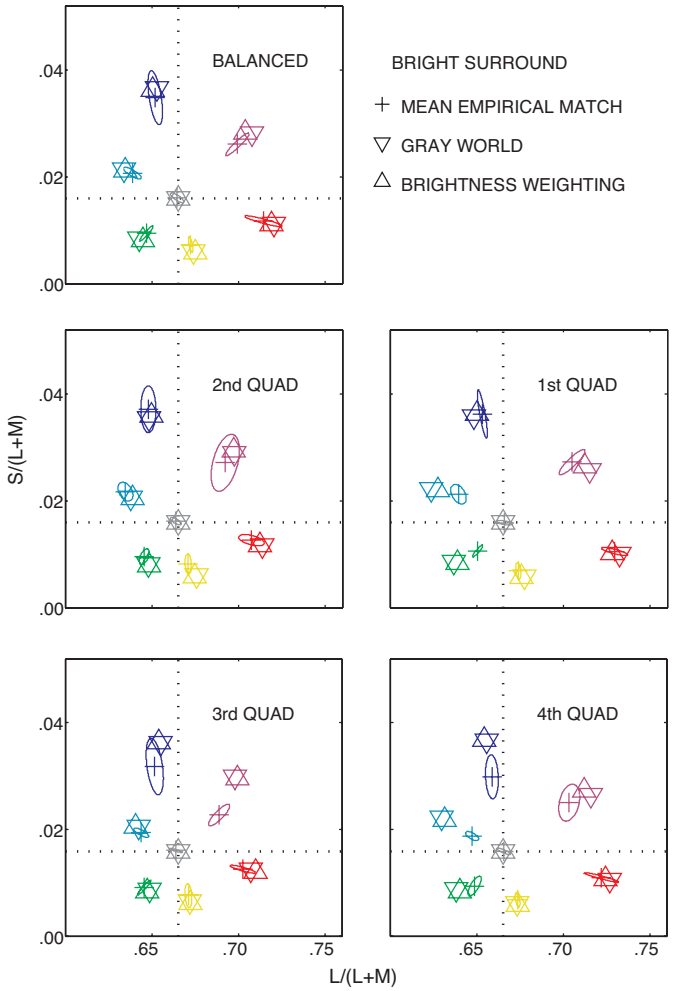

Figure 10. Mean chromaticities of the Match spotlights (+), and predictions from a gray-world model (▽), and a model that gives greater weight to the brightest materials (△). Note that these models are different from the ones in Figures 6 and 8.

Model 3: Illuminant-based color estimation for filters

The increased accuracy of spotlight matches in Experiment 3 compared to Experiment 1 demonstrates that observers are utilizing the extra information available from the exposed regions. It is clear that the simple illuminant estimation models described earlier will not provide good fits to the data from Experiment 3. In addition, when the surround is brighter than the spotlighted region, it is obvious that the spotlight is not being added to the background illuminant. To be consistent with the optics of the situation, we conjecture that observers first estimate the illuminant $E_c(\lambda)$ on the exposed region of the chromatic background, and then assume that the spotlight $P_j(\lambda)$ is equal to $F_j(\lambda)^* E_c(\lambda)$, where '*' is wavelength-by-wavelength multiplication, and $F_j(\lambda)$ is the spectrum that filters the illuminant common to overlaid and exposed regions. If the estimates $\hat{P}_j(\lambda)$ and $\hat{E}_c(\lambda)$ were available, then observers could simply estimate $\hat{F}_j(\lambda) = \hat{P}_j(\lambda) / \hat{E}_c(\lambda)$, where '/' is wavelength-by-wavelength division. It is unlikely that observers could estimate these complete spectra. However, these spectral estimates are not necessary because the filter cone-coordinates can be estimated in a simpler manner based on the empirical observations that illuminants and filters overlaid on everyday materials do not alter the rank orders of L, M, and S cone absorptions (Dannemiller, 1993; Foster & Mascimento, 1994; Nascimento & Foster, 1997; Zaidi et al., 1997; Westland & Ripamonti, 2000; Zaidi, 2001; Khang & Zaidi, 2002). In other words, cone-catches under equal-energy light and cone-catches under another light or filter are related by the same multiplicative constant for all materials. The observer can thus estimate $\left[L_c(\hat{F}_j),\ M_c(\hat{F}_j),\ S_c(\hat{F}_j)\right]$ from the ratios $\left[L_c(\hat{P}_j)/L_c(\hat{E}_c),\ M_c(\hat{P}_j)/M_c(\hat{E}_c),\ S_c(\hat{P}_j)/S_c(\hat{E}_c)\right]$. [*Note that without this assumption, L(F) will be equal to L(P/E), not L(P)/L(E)*]. $\left[L_c(\hat{P}_j),\ M_c(\hat{P}_j),\ S_c(\hat{P}_j)\right]$ are estimated from Equations 9-11, and $L_c(\hat{E}_c)$, $M_c(\hat{E}_c)$, $S_c(\hat{E}_c)$ from Equations 16-18 (Note that for Experiment 3, $E(\lambda)$ is 5 times the value for Experiment 2).

The linking hypothesis for the spotlight matches is that the observer sets $P_m(\lambda)$ on the achromatic side, so that

$$L_a(F_m) = L_c(\hat{F}_j) \tag{33}$$

$$M_a(F_m) = M_c(\hat{F}_j) \tag{34}$$

$$S_a(F_m) = S_c(\hat{F}_j) \tag{35}$$

where

$$L_a(F_m) = L_a(P_m)/L_a(E_a) \tag{36}$$

$$M_a(F_m) = M_a(P_m)/M_a(E_a) \tag{37}$$

$$S_a(F_m) = S_a(P_m)/S_a(E_a). \tag{38}$$

This implies that cone-absorptions for P_m can be obtained by

$$L_a(P_m) = \frac{L_c(\hat{P}_j)}{L_c(\hat{E}_c)} \cdot L_a(\hat{E}_a) \tag{39}$$

$$M_a(P_m) = \frac{M_c(\hat{P}_j)}{M_c(\hat{E}_c)} \cdot M_a(\hat{E}_a) \tag{40}$$

$$S_a(P_m) = \frac{S_c(\hat{P}_j)}{S_c(\hat{E}_c)} \cdot S_a(\hat{E}_a) \quad (41)$$

where the cone estimates for E_a the illuminant on the achromatic side are given by Equations 29-31. (Note that for Experiment 3, $E(\lambda)$ is 5 times the value for Experiment 2.)

The predicted values of $[L_a(P_m),\ M_a(P_m),\ S_a(P_m)]$ were converted to MacLeod-Boynton chromaticities and compared to the empirical matches from Figure 9, which are replotted as plusses on the same axes in Figure 10 . The other symbols near the plusses show the model predictions for $n = 0$ and 10 (downward and upward pointing triangles, respectively). Note that there are no free parameters in this model. The value of n which determines the selectivity of brightness weighting is fixed for each model. Many of the points from the gray-world ($n = 0$) hypothesis come close to the data points, particularly to the empirical matches that were close to veridical. The $n = 0$ model here is mathematically identical to the model for equating mean cone-ratios that was presented in Khang and Zaidi (2002), so the models in this work provide a perceptual interpretation for the mechanistic models in Khang and Zaidi (2002). The predictions for $n = 1$ were very similar to those for $n = 0$. The predictions of the brightness-weighted model ($n = 10$) do not differ greatly from the gray-world model, but do provide a slightly better fit to some data points. The predictions for $n = 100$ were very similar to that for $n = 10$. The models' predictions are generally close to the veridical matches; therefore, the predominant discrepancies from the predictions occur for matches that were far from veridical, and in these cases the matched chromaticity is less saturated than the predicted chromaticity.

Conclusions

This study presents measurements of illuminant color matching by human observers. The results show that when only one illuminant is in the field of view, despite the rich chromatic information provided by a spotlight traversing materials of diverse spectral reflectance, estimates of illuminant color are seriously biased by the chromaticities of the illuminated surfaces. We show that a gray-world model cannot be rejected as an adequate explanation for the biased matches. A model that gives greater weights to the brightest surfaces provides a similar fit to the data. The models have no free parameters, and we do not consider nonlinear functions, so the similarities between predictions and data indicate that, for flat matte surfaces, simple combinations of the cone-absorptions available from the displays are the important factors in illuminant color perception.

The results of the second and third experiments show that when the surround of a spotlight is illuminated by a second light, spotlight matching is more accurate, and is close to veridical in most conditions for bright surrounds. We present models based on first estimating the illuminant colors for the spotlighted and exposed regions using the same rules as for single illuminants, and then discounting the illuminant common to the two regions by using equations that are consistent with the optics of the situations. For the case where the spotlight is brighter than the surrounding illuminant, the discounting is done through an additive model; whereas, for the case where the surrounding illuminant is brighter than the spotlight, the discounting is done through a multiplicative model. These models provide adequate fits to the data.

The results of our first experiment can be compared to those of the second experiment of Linnell and Foster (2002). They asked observers to match the simulated steady illuminant on two 7.0-deg square backgrounds consisting of 49 Munsell reflectances each. One background reflected more light in the orange region but included a white surface; the match background was unbiased in color. They manipulated patch sizes from one pixel to 1.0 deg. Their main result was that illuminant matches were always much closer to the space-averaged color than to the color of the brightest patch. The moving spotlight in our study provides a much more compelling scission between illuminant and background colors, similar to the improved scission for moving filters documented by D'Zmura, Rinner, and Gegenfurtner (2000) and Khang and Zaidi (2002). In addition, we used a number of different biased colored backgrounds to test whether the estimation of spotlight was better when the spectra of the light and background materials were similar than when they were dissimilar, and our model (Equations 9-15) allows for testing a larger range of possibilities. Despite these differences, the results of both experiments are substantially in accord.

Nascimento and Foster (1997, 2000) have shown that the discrimination of illuminant changes from non-illuminant changes is mediated by spatial ratios of cone excitations. The results of Experiments 2 and 3 show that spatial ratios of cone excitations can also function to identify the same illuminant across disparate backgrounds, but only in the presence of a brighter second illuminant.

Estimates of illuminant cone coordinates can also be obtained indirectly by measuring the appearance of illuminated and veiled surfaces (Brainard & Wandell, 1991; Brainard, 1998; Hagedorn & D'Zmura, 2000). These estimates assume a two-step framework for human color vision, where the image data is processed to yield an estimate of the illuminant, and then this estimate is used to correct the light reflected from each image location to yield a surface color. The framework has only been directly tested for achromatic situations, and there it has been falsified (Rutherford & Brainard, 2002). Using a color categorization procedure, Smithson and Zaidi (2004) showed that adaptation to an illuminant can lead to appearance-based color constancy, but that it is based on spatially local processes rather than a space-averaged mean. This suggests that the per-

ceived colors of spatially extended illuminants are not the functional factor in perceptually discounting changes of illuminants.

In summary, the results of this study show that the presence of a second illuminant in a scene is important for accurate color estimation of an illuminant. When a spotlight is the only illuminant in the scene, the chromaticity of a matched spotlight tends to be set near the mean chromaticity of the brightest surfaces.

Acknowledgments

Portions of this work were presented at the conference of the Vision Sciences Society, 2002, in Sarasota, FL. We would like to thank Lars Chittka, Justin Marshall, Larry Maloney, and Cuopio University for providing the reflectance functions, and Yan Chen, Long Tran, and Brian Williams for patient observations. This work was supported by National Eye Institute Grant EY07556 to QZ.

Commercial relationships: none.
Corresponding author: Byung-Geun Khang.
Email: b.g.khang@phys.uu.nl.
Address: Helmholtz Institute, Utrecht University, Utrecht, The Netherlands.

References

Adelson, E. H., & Pentland, A. P. (1991). The perception of shading and reflectance. In B. Blum (Ed.), *Channels in the visual nervous system: Neurophysiology, psychophysics and models.* London: Freund Publishing House, Ltd.

Beck, J. (1959). Stimulus correlates for the judged illumination of a surface. *Journal of Experimental Psychology, 58*(4), 267-274. [PubMed]

Brainard, D. H. (1998). Color constancy in the nearly natural image. 2. Achromatic loci. *Journal of the Optical Society of America A, 15*(2), 307-325. [PubMed]

Brainard, D. H, & Freeman, W. T. (1997). Bayesian color constancy. *Journal of the Optical Society of America, A, 14*(7), 1393-1411. [PubMed]

Brainard, D. H., & Wandell, B. A. (1991). A bilinear model of the illuminant's effect on color appearance. In M. S. Landy and A. J. (Eds.), *Movshon computational models of visual processing.* Cambridge, MA: MIT Press.

Buchsbaum, G. (1980). A spatial processor model for object colour perception. *Journal of the Franklin Institute, 310*, 1-26.

Chittka, L., Shmida, A., Troje, N., & Menzel, R. (1994). Ultraviolet as a component of flower reflections, and the colour perception of Hymenoptera. *Vision Research, 34*, 1489-1508. [PubMed]

Dannemiller, J. L. (1993). Rank orderings of photoreceptor photon catches from natural objects are nearly illuminant-invariant. *Vision Research, 33*, 131-140. [PubMed]

D'Zmura, M., & Iverson, G. (1993). Color constancy. II. Results for two-stage linear recovery of spectral descriptions for lights and surfaces. *Journal of the Optical Society of America A, 10*(10), 2166-2180. [PubMed]

D'Zmura, M., & Iverson, G. (1994). Color constancy. III. General linear recovery of spectral descriptions for lights and surfaces. *Journal of the Optical Society of America A, 11*(9), 2398-2400. [PubMed]

D'Zmura, M., & Lennie, P. (1986). Mechanisms of color constancy. *Journal of the Optical Society of America A, 3*, 1662-1672. [PubMed]

D'Zmura, M., Rinner, O., & Gegenfurtner, K. R. (2000). The colors seen behind transparent filters. *Perception, 29*, 911-926. [PubMed]

Finlayson, G. D., Hubel, P. M., & Hordley, S. (1997). Color by correlation. In *Proceedings of the Fifth Color Imaging Conference* (pp. 6-11). Springfield, VA: Society for Imaging Science and Technology.

Forsyth, D. A. (1990). A novel algorithm for color constancy. *International Journal of Computer Vision, 5*, 5-36.

Foster, D. H., & Nascimento, S. M. (1994). Relational colour constancy from invariant cone excitation ratios. *Proceedings of the Royal Society of London B, 257*, 115-21. [PubMed]

Gegenfurtner, K. R., Kiper, D. C., & Levitt, J. B. (1997). Functional properties of neurons in macaque area V3. *Journal of Neurophysiology, 77*(4), 1906-1923. [PubMed]

Gilchrist, A., & Jacobsen, A. (1984). Perception of lightness and illumination in a world of one reflectance. *Perception, 13*(1), 5-19. [PubMed]

Golz, J., & MacLeod, D. I. (2002). Influence of scene statistics on colour constancy. *Nature, 415*(6872), 637-640. [PubMed]

Hagedorn, J., & D'Zmura, M. (2000). Color appearance of surfaces viewed through fog. *Perception, 29*, 1169-1184. [PubMed]

Helmholtz, H. von. (1962). *Helmoltz's treatise on physiological optics* (J. P. Southall, Ed.). New York: Dover. (Original work published 1866)

Judd, D. B. (1961). A five-attribute system of describing visual appearance. *American Society for Testing and Materials Special Technical Publication, 297*, 1-15.

Kardos, L. (1929). Die "Konstanz" phänomenaler Dingmomente. *Beitr Problemgeschichte Ps* (Bühler Festschr) (pp. 1-77). Jena: Fischer.

Katz, D. (1935). *World of colour*. New York: Johnson Reprint Corp.

Khang, B. -G., & Zaidi, Q. (2002). Accuracy of color scission for spectral transparencies. *Journal of Vision, 2*(6), 451-466, http://journalofvision.org/2/6/3, doi:10.1167/2.6.3. [PubMed][Article]

Kiper, D. C., Fenstemaker, S. B., & Gegenfurtner, K. R. (1997). Chromatic properties of neurons in macaque area V2. *Vision and Neuroscience, 14*(6), 1061-1072. [PubMed]

KodakCC (1962). Kodak Wratten filters: For scientific and technical use. Rochester, NY: Eastman Kodak Co.

Koffka, K. (1935). *Principles of Gestalt psychology*. New York: Harcourt & Brace.

Krauskopf, J., Williams, D. R., & Heeley, D. W. (1982). Cardinal directions of color space. *Vision Research, 22*(9), 1123-1131. [PubMed]

Land, E. H. (1986). Recent advances in retinex theory. *Vision Research, 26*, 7-21. [PubMed]

Lee, H.-C. (1986). Method for computing the scene illuminant chromaticity from specular highlights. *Journal of the Optical Society of America A, 3*, 1694-1699. [PubMed]

Lehmann, T. M., & Palm, C. (2001). Color line search for illuminant estimation in real-world scenes. *Journal of the Optical Society of America A, 18*(11), 2679-2691. [PubMed]

Lennie, P., Krauskopf, J., & Sclar, G. (1990). Chromatic mechanisms in striate cortex of macaque. *Journal of Neuroscience, 10*(2), 649-669. [PubMed]

Linnell, K. J., & Foster, D. H. (2002). Scene articulation: Dependence of illuminant estimates on number of surfaces. *Perception, 31*, 151-159. [PubMed]

Lenz, R., Osterberg, M., Hiltunen J., Jaaskelainen, T., & Parkkinen, J. (1996). Unsupervised filtering of color spectra. *Journal of the Optical Society of America*, A, 13, 1315-1324.

MacLeod, D. I. A., & Boynton, R. M. (1979). Chromaticity diagram showing cone excitation by stimuli of equal luminance. *Journal of the Optical Society of America, A, 69*, 1183-1186. [PubMed]

MacLeod, D. I. A., & Golz, J. (2003). A computational analysis of colour constancy. In R. Mausfeld & D. Heyer (Eds.), *Colour vision: From light to object*. Oxford: Oxford University Press.

Maloney, L .T., & Wandell, B. A. (1986). Color constancy: A method for recovering surface spectral reflectance. *Journal of the Optical Society of America A, 3*(1), 29-33. [PubMed]

Marshall, N. J. (2000). Communication and Camouflage with the same 'bright' colours in reef fishes. *Philosophical Transactions of the Royal Society of London B, 355*, 1243-1248. [PubMed]

Nascimento, S. M., & Foster, D. H. (1997). Detecting natural changes of cone-excitation ratios in simple and complex coloured images. *Proceedings of the Royal Society of Londo, B, 264*, 1395-1402. [PubMed]

Nascimento, S. M., & Foster, D. H. (2000). Relational color constancy in achromatic and isoluminant images. *Journal of the Optical Society of America, A, 17*(2), 225-231. [PubMed]

Rutherford, M. D., & Brainard, D. H. (2002). Lightness constancy: A direct test of the illumination-estimation hypothesis. *Psychological Sciences, 13*(2), 142-149. [PubMed]

Smith, V. C., & Pokorny, J. (1975). Spectral sensitivity of the foveal cone photopigments between 400 and 700 nm. *Vision Research, 15*, 161-171. [PubMed]

Smithson, H., & Zaidi, Q. (2004). Color constancy in context: Roles of local adaptation and reference levels. *Journal of Vision, 4*(9), 693-710, http://journalofvision.org/4/9/3/, doi:10.1167/4.9.3. [PubMed][Article]

Tominaga, S., Ebisui, S., & Wandell, B. A. (2001). Scene illuminant classification: Brighter is better. *Journal of the Optical Society of America A, 18*(1), 55-64. [PubMed]

Tominaga, S., & Wandell, B. A. (1989). Standard surface-reflectance model and illuminant estimation. *Journal of the Optical Society of America A, 6*, 576-584.

Vrhel, M., Gershon, R., & Iwan, L. S. (1994). Measurement and analysis of object reflectance spectra. *Color Research and Application, 19*, 4-9.

Webster, M. A., & Mollon, J. D. (1997). Adaptation and the color statistics of natural images. *Vision Research, 37*, 3283-3298. [PubMed]

Westland, S., & Ripamonti, C. (2000). Invariant cone-excitation ratios may predict transparency. *Journal of the Optical Society of America A, 17*, 255-264. [PubMed]

Woodworth, R. S. (1938). *Experimental psychology*. London: Methuen.

Yang, J., -N., & Maloney, L. T. (2001). Illuminant cues in surface color perception tests of three candidate cues. *Vision Research, 41*, 2581-2600. [PubMed]

Zaidi, Q. (1998). Identification of illuminant and object colors: Heuristic-based algorithms. *Journal of the Optical Society of America, 15*(7), 1767-1776. [PubMed]

Zaidi, Q. (2001). Color constancy in a rough world. *Color Research and Application, 26*, S192-S200.

Zaidi, Q., Spehar, B., & DeBonet, J. (1997). Color constancy in variegated scenes: Role of low-level mechanisms in discounting illumination changes. *Journal of the Optical Society of America A, 14*, 2608-2621. [PubMed]

Zaidi, Q., Spehar, B., & DeBonet, J. (1998). Adaptation to textured chromatic fields. *Journal of the Optical Society of America A*, 15, 23-32. [PubMed]

Zavagno, D. (1999). Some new luminance-gradient effects. *Perception, 28*(7), 835-838. [PubMed]